Microstructures and Hardness of as-cast C, Ta or Ti or Hf of Zr-containing Cr-rich Niobium-based Alloys Candidate for Uses at Elevated Temperatures

Patrice Berthod, Mélissa Léglise, Ghouti Medjahdi

Thermal Science and Engineering (2018) Volume 1
doi:10.24294/tse.v1i4.842

Microstructures and Hardness of as-cast {C, Ta or Ti or Hf of Zr}-containing Cr-rich Niobium-based Alloys Candidate for Uses at Elevated Temperatures

Patrice Berthod*, Mélissa Léglise, Ghouti Medjahdi

Institut Jean Lamour, University of Lorraine, Faculty of Sciences and Technologies, Vandoeuvre-lès-Nancy 54506, France, E-mail : patrice.berthod@univ-lorraine.fr

ABSTRACT

Four alloys based on niobium and containing about 33wt.%Cr, 0.4wt.C and, in atomic content equivalent to the carbon one, Ta, Ti, Hf or Zr, were elaborated by classical foundry under inert atmosphere. Their as-cast microstructures were characterized by X-ray diffraction, electron microscopy, energy dispersion spectrometry and while their room temperature hardness was specified by Vickers indentation. The microstructures are in the four cases composed of a dendritic Nb-based solid solution and of an interdendritic $NbCr_2$ Laves phase. Despite the MC-former behavior of Ta, Ti, Hf and Zr usually observed in nickel or cobalt-based alloys, none of the four alloys contain MC carbides. Carbon is essentially visible as graphite flakes. These alloys are brittle at room temperature and hard to machine. Indentation shows that the Vickers hardness is very high, close to $1000HV_{10kg}$. Indentation lead to crack propagation through the niobium phase and the Laves areas. Obviously no niobium-based alloys microstructurally similar to high performance MC-strengthened nickel-based and cobalt-based can be expected. However the high temperature mechanical and chemical properties of these alloys remain to be investigated.

***Keywords*:** Niobium-based alloys; High chromium content; MC carbide-former elements; Microstructures; Hardness

1. Introduction

Looking for service temperatures higher and higher to increase performance and efficiency leads to the necessity of developing alloys beyond the best present superalloys as the single crystalline γ/γ' nickel-based ones[1-3]. Many solutions are currently explored such as cobalt-based especially rich in heavy elements[4,5] or reinforced by γ' precipitation[6,7]. Refractory versions of the new concept of High Entropy Alloys, rich in heavy elements, are also being considered[8]. In another way the metallurgical principles exploited in the oldest superalloys as the carbide-strengthened chromia-forming equiaxed cast alloys based on nickel or cobalt may be also revisited with new elements and new hardening particles. This is, for instance, what was recently done with conventionally cast chromium-rich cobalt-based[9,10], iron-based[11] and nickel-based[12] alloys strengthened by eutectic HfC carbides. Such alloys, taking back the commonly used base elements of the current superalloys, and in which chromium / tungsten or tantalum carbides are replaced by exotic but much more stable carbides, showed very interesting mechanical properties at temperatures as high as 1100°C[13] and even 1200°C[14]. Various types of MC carbides were very recently successfully obtained as script-like eutectic carbides in polycrystalline cobalt-based[15] and nickel-based[16] alloys elaborated by classical foundry, with as result potential creep resistance at elevated temperature (up to 1200°C). To progress in term of temperature level in the field of the mechanical properties, one can now think to replace the base elements cobalt, nickel or iron, by a very refractory one: niobium (melting point equal to 2469°C[17]). This element takes part to the current superalloys, for example as γ' -former beside Al, but it can be also used as base element for some refractory metallic alloys[18,19]. Thus combining a niobium matrix,

doi: 10.24294/tse.v1i4.842

rich in chromium to achieve resistance not only to high temperature oxidation but also against corrosion by various aggressive molten substances (sulfides, CMAS, glasses…)[20], and an interdendritic carbide often recent results concerning the morphology and thermodynamic high stability at elevated temperature obtained in Co-, Fe- or Ni-based alloys, four MC-former elements were selected: Ta, Ti, Hf and Zr.

These four elements are often encountered in the chemical compositions of refractory metallic materials, either as alloying element, or as base one. Indeed, tantalum – elsewhere used in some famous cast cobalt-based superalloys[1,2] – may form TaC carbides favorable to high strength thanks to their initial script-like morphology and their rather high stability at high temperature (example of the famous Mar-M509). These properties may be also brought by the TiC carbides, formed with titanium which is also a γ'-former element and which can be used as base element as in the wellknown Ti-6Al-4V[21]. Hf, which led to the high performance directionally solidified DS200-Hf alloy[22] and which may serve to configure microstructures and properties of some alloys[23,24], allow obtaining script-like MC carbides especially stable at elevated temperature in term of both morphology and volume fraction[9-12], whatever the base element among cobalt, nickel and iron. Zirconium, sometimes added to cobalt-based or nickel-based superalloys[25,26], can be also met as base of refractory alloys such as the Zircaloy-4[27].

In this work, one wished, by keeping the conventional foundry process, to go beyond nickel, cobalt and iron-based alloys, by investigating these four metallurgical systems: Nb-32.5 wt.% Cr-0.39 wt.% C- x M, with x M = 5.90 wt.% Ta ("NbCrC-TA" alloy), 1.56 wt.%Ti ("NbCrC-TI" alloy), 5.80 wt.% Hf ("NbCrC-HF" alloy) or 2.96 wt.% Zr ("NbCrC-ZR" alloy). The weight contents in M are calculated to respect the atomic parity of C and M to promote the formation of exclusively MC carbides. This involved first the possibility or not of elaboration by melting and solidification, the characterization of the as-cast microstructures of the obtained alloys, and to start specifying their machinability and room temperature properties by indentation tests.

2. Experimental

Preparation of the alloys and foundry process

The preparation of the four alloys started by weighing with a precision balance (accuracy: ±0.1 mg) small parts of pure elements (Nb, Cr, Ta, Ti, Hf, Zr: Alfa Aesar, purity > 99.9%, C: pure graphite) for obtaining total charges of about 10 grams.

For each charge the pure elements were placed and mixed together in the metallic crucible of a High Frequency Induction Furnace (CELES, France). During operation, this crucible, made of pure copper, was cooled by the internal circulation of fresh water. A silica tube was then placed around the crucible, this allowing the isolation of the melting chamber from air laboratory. A pump allowed reaching an internal pressure of about 5 × 10^{-2} mbars, before pure argon was introduced in the chamber until representing about 800 millibars. This sequence, pumping followed by Ar introduction, was repeated three times. Finally Ar was introduced a last time for obtaining an internal atmosphere of about 300 mbars. The charge and the fusion chamber were thus ready for carrying out heating and melting. Heating was realized by applying an increasing voltage until reaching 2.5 kV. After thermal homogenization of the still solid parts, a new increase led to 5 kV (melting of the alloy), voltage maintained during 5 minutes (total melting and chemical homogenization of the molten alloy). Cooling was achieved by first progressively decreasing voltage down to 0 (solidification of the alloy into a solid but hot ingot), and by about thirty minutes of cooling of the obtained ingot in contact with the cold copper of the crucible. Without disassembling the apparatus the whole operation described just before was made a second time, in order to be really sure that the alloy was veritably totally melted and homogenized, to avoid discovering any not-melted particles after cutting.

Metallography samples preparation, microstructure and hardness characterization

The obtained ingots were cone-like shaped, with a mass of about 40 grams, a diameter of about 20mm and a height of about 20 mm too. Each ingot was cut in two equal parts using a metallographic saw (Abrasimet 5000, Buelher) and a thin abrasive SiC blade under cooling liquid flow. The behavior of the ingots during this preliminary operation may give first qualitative indications concerning levels of hardness and toughness,

possible machining difficulties, room temperature brittleness…

The two halves were optically observed. One of them was embedded in a cold resin mixture (ESCIL, France), then ground and polished to obtain metallography samples for the microstructure observations. Grinding was carried out by using successive grades of SiC paper (from 120 to 1200). After ultrasonic cleaning and water and alcohol washing, the samples were polished with textile enriched with 1µm hard particles until obtaining a surface state as mirror-like as possible.

The microstructures of the obtained alloys were first characterized by X-ray diffraction, using a Philips X'Pert Pro diffractometer (wavelength = 1.5406 Å, Cu K). Second the alloys were observed by electron microscopy using a Scanning Electron Microscope (SEM), model JEOL JSM 6010-LA. This was done in the Back Scattered Electrons (BSE) mode, under a voltage equal to 15kV. The general chemical composition was controlled using the Energy Dispersion Spectrometry device attached to the SEM. This one was also involved in the spot measurements of the chemical composition of each seen phase. When possible image analysis was applied to value the surface fraction of each seen phase, using the tool included in the Photoshop CS software of Adobe.

The alloys were also subjected to indentation tests, using a Testwell Wolpert machine. This was done according to the Vickers method, for a 10kg load. About ten measurement results allowed calculating an average hardness value and a standard deviation one for each alloy. The indented samples were observed using the same SEM but in Secondary Electrons mode to observe the obtained hardness imprint and the stat of their neighborhood, notably the possible cracks resulting from the indentation tests.

3. Results and discussion

Behaviors of the alloys during cutting

Macrophotographs of the two (or three) parts issued from the cutting operation are displayed in **Figure 1**. In no case cutting finished without a final sudden rupture. This one was seemingly brittle, as suggested by the aspects of the rupture surfaces.

Figure 1; Macrographs of the four ingots after final rupture at the end of cutting**.**

These first observations let think to future compulsory work to significantly improve room temperature ductility and toughness (e.g. by addition in small contents of elements such as boron of example) to allow envisaging mechanical subtracting manufacturing for real pieces which may be additionally of greater dimensions.

Generalities about the as-cast microstructures of the four alloys

After embedding and polishing the samples of the as-cast alloys were examined by electron microscopy. Four typical low magnification (×250) SEM/BSE micrographs illustrating the as-cast microstructures of the four alloys are provided in **Figure 2**. The four alloys are obviously constituted of two main constituents: a white one and of a grey one. The white phase is more (the Ta, Ti or Nb-containing alloys) or less (the Hf-containing one) dendritic, while the grey constituent occupies the interdendritic spaces. This constituent seems double-phased, composed of white phase mixed with a dark grey phase. In addition to these main phase or constituent, some very fine black particles can be seen (further examinations will reveal the presence of fine particles very rich in carbon), as well as, exclusively in

the Ti-containing alloy, a coarse pale grey phase (this will be further identified as a niobium carbide).

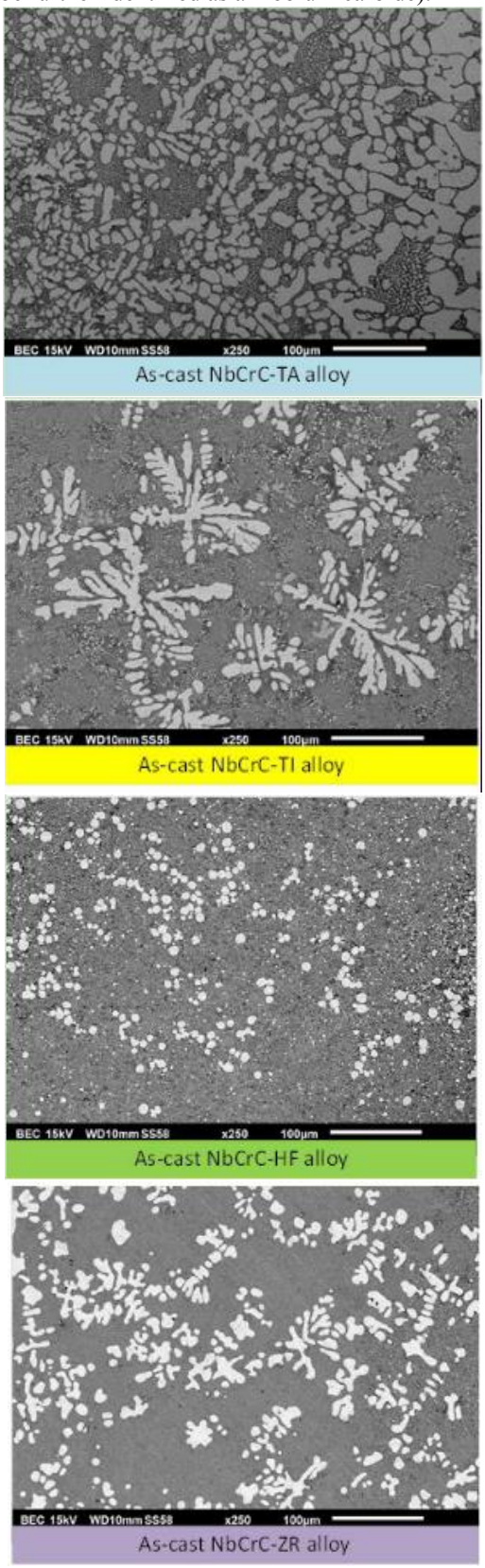

Figure 2; SEM/BSE micrographs illustrating the general as-cast microstructures of the four alloys**.**

These microstructures let thinking that solidification started by nucleation and growth of the white phase and possibly finished with a eutectic solidification part leading to the interdendritic constituent made of white phase and dark grey phase.

Microstructure of the as—cast NbCrC-TA alloy

The metallic surfaces of the prepared metallographic samples were subjected to both X-ray diffraction, high magnification (×1000) SEM/BSE observations and spot EDS analyses. In the case of the tantalum-containing alloy the obtained results are illustrated in **Figure 3** by a diffractogram and an electronic micrograph. The two characterization ways indicated that this alloy contains:

- A body centered cubic (BCC) niobium solid solution containing about 14-15 wt.% of chromium and slightly near 8 wt.% of tantalum
- An intermetallic $NbCr_2$ phase containing itself about 8 wt.% of Ta
- Small particles rich in carbon, with a more or less elongated shape.

This is the white phase which is the Nb solid solution. It is first constituted of the coarse dendrites, and second of the numerous small and more or less blocky particles mixed with the dark grey $NbCr_2$ compound in the interdendritic areas. This $NbCr_2$ compound may be present as two distinct varieties: a cubic one (space group: Fd-3m) and a hexagonal one (space group: P63/mmc), according to these XRD results. But it is true that many of the major diffraction peaks corresponding to the hexagonal $NbCr_2$ specie may be also attributed to a Nb_2C carbide. Careful SEM examination did not allow finding such niobium di-carbide, at least in quantity high enough to lead to visible XRD peaks. It can be thus considered that the two $NbCr_2$ are simultaneously present in this first alloy.

Concerning the third present phase, the carbon-rich particles, their shapes look like the lamellar or blocky possible ones of graphite, or the acicular or compact possible one of chromium carbides; these particles were only detected by SEM/BSE observations, identified as particularly rich in C by EDS; unfortunately they too small size did not allow determining their exact nature, neither by SEM/EDS (and even Electron Probe Micro-Analysis), nor by XRD because they are not

present in surface fractions high enough.

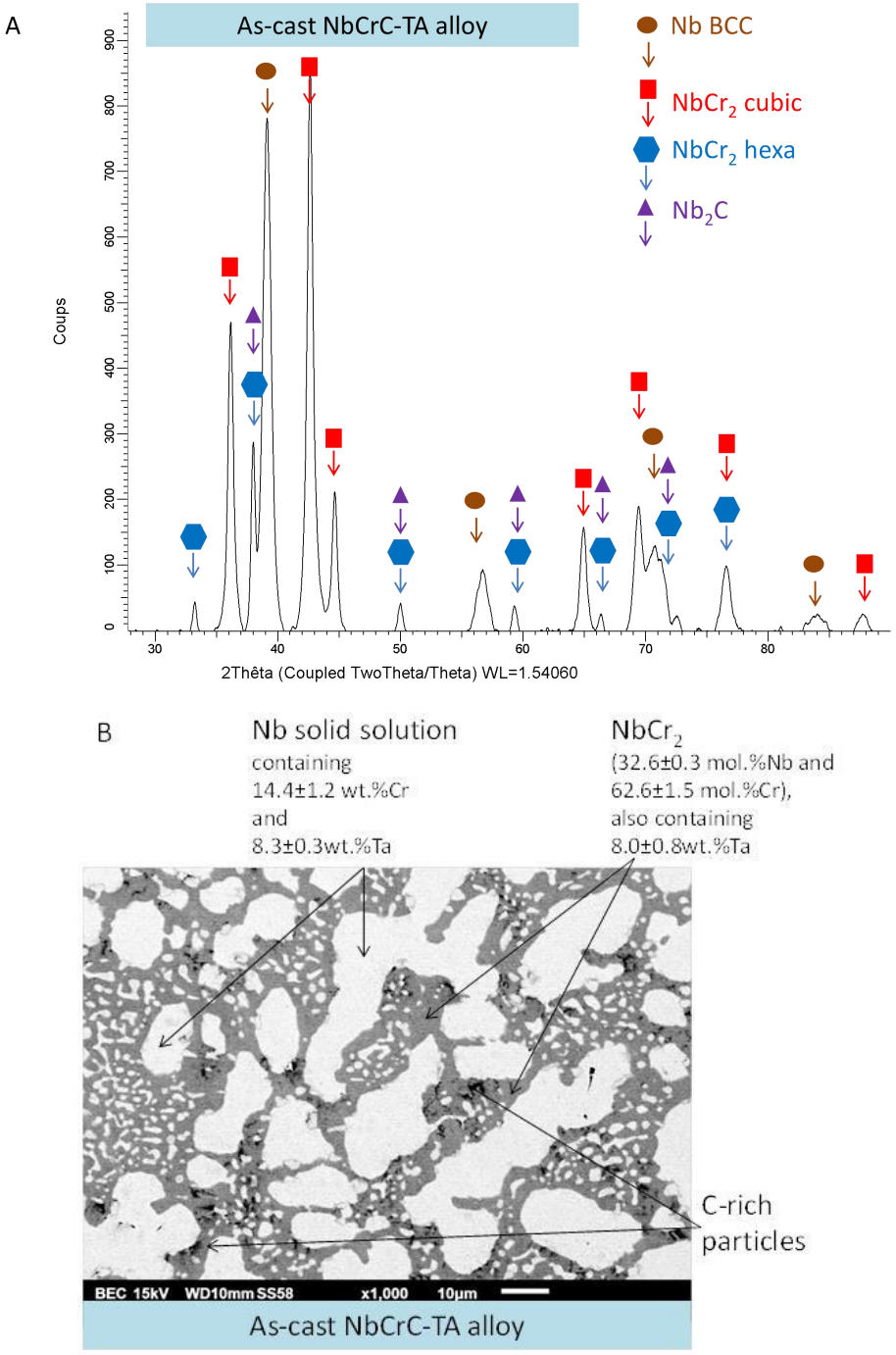

Figure 3; Ta-containing alloy: XRD diffractometer (A) and detailed view of its microstructure (B) with identification of the present phases (SEM/BSE micrograph)**.**

Microstructure of the as—cast NbCrC-TI alloy

According to the obtained XRD diffractogram, SEM/BSE observations and EDS analyses (Fig. 4), the titanium-containing alloy is composed of:

- Dendrites and interdendritic zones of a BCC Nb solid solution containing about 17 wt.% of chromium and 1.5 wt.% of titanium,
- Colonies of blocky Nb_2C carbides (grey) in which 4 wt.% of titanium is also present,
- An intermetallic $NbCr_2$ phase containing itself about 1.4 wt.% of Ti mixed with the Nb solid solution in the interdendritic spaces,
- Dispersed small carbon-rich particles, seemingly present in less quantities than in the Ta-containing

alloy.

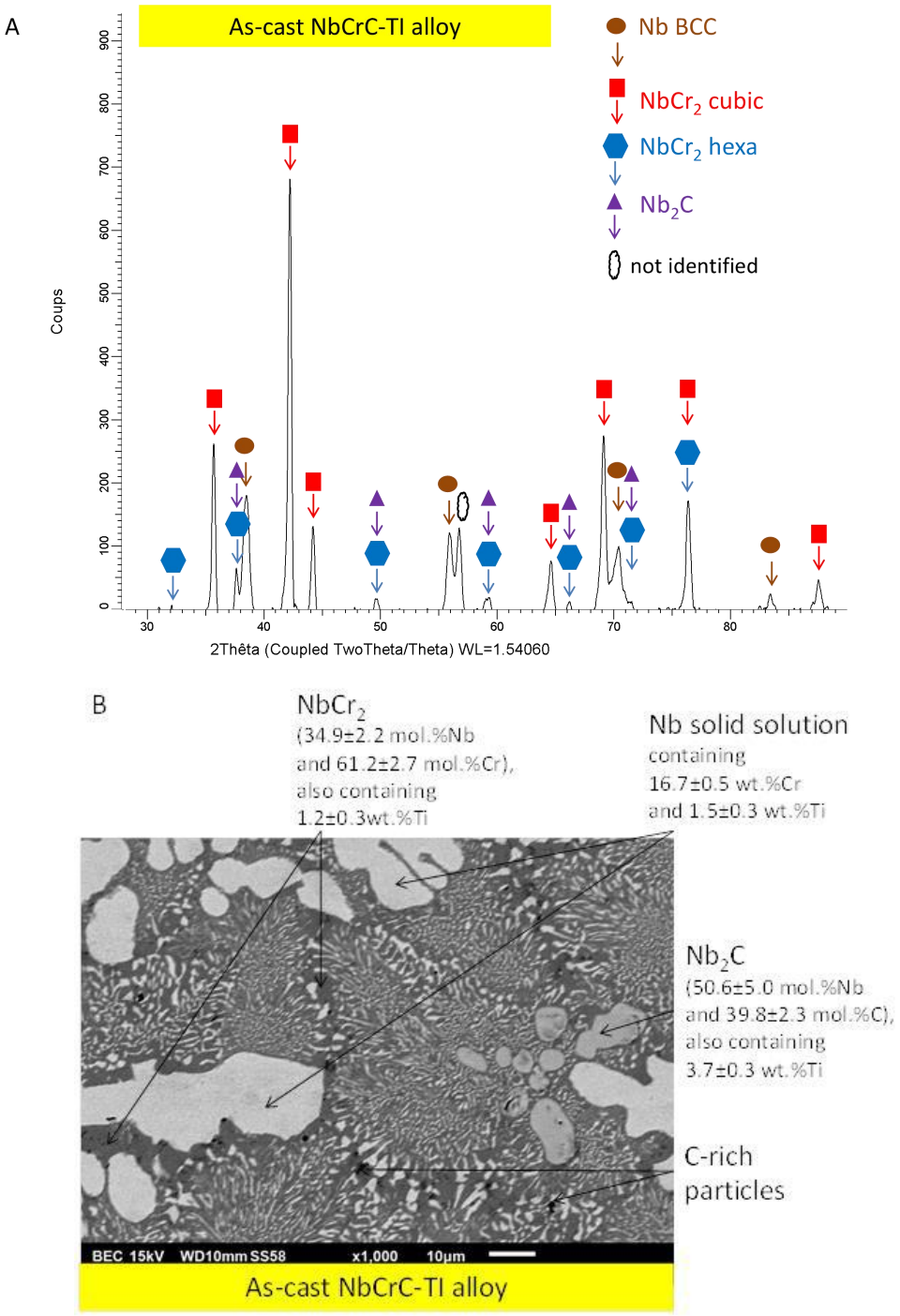

Figure 4; Ti-containing alloy: XRD diffractometer (A) and detailed view of its microstructure (B) with identification of the present phases (SEM/BSE micrograph)**.**

The dendrites and the white interdendritic particles mixed with the grey phase are composed of the same solid solution as in the Ta-containing alloy, but with the presence of Ti instead Ta in solid solution. Another difference from this previous alloy is the presence here of a carbide phase, not formed with Ti but with Nb, seemingly with the M_2C stoichiometry and not MC, as shown by both the XRD diffractogram and by several spot EDS analyses. The presence of these Nb_2C carbides appears to be consistent with the much lower quantity of carbon-rich particles (chromium carbides or graphite) by comparison with the Ta-containing alloy. Concerning the $NbCr_2$ phase, the presence of the cubic variety is demonstrated by the corresponding XRD peaks, but it

appears difficult to state about a possible simultaneous presence of the hexagonal variety because of the existence of the Nb_2C carbide which shares the same DRX peaks.

Microstructure of the as—cast NbCrC-ZR alloy

The microstructure of the zirconium-containing alloy, as suggested by the same types of analyze results (**Figure 5**) as the Ta-containing one, is constituted of:

- Dendrites of a BCC Nb solid solution containing about 16 wt.% of chromium and 2.2 wt.% of zirconium,
- An intermetallic $NbCr_2$ phase containing itself about 1.2 wt.% of Zr mixed with Nb solid solution in the interdendritic spaces to form a finely structured eutectic compound; the Nb_2C carbides being obviously absent in the microstructures (SEM/BSE examinations) the $NbCr_2$ phase exists with two crystalline structures: cubic and hexagonal (shown by the corresponding XRD peaks)
- Carbon-rich fine particles in rather low quantities by comparison with the two former alloys.

Microstructure of the as—cast NbCrC-HF alloy

This fourth alloy is much more original **(Figure 6**). One finds again the same eutectic compound made of BCC Nb solid solution (with again about 15 wt.% Cr, and now 3 wt.% Hf) and of $NbCr_2$ phase (containing 6 wt.% Hf). In contrast with the three previous ones, the Nb solid solution exists not as dendrites and as interdendritic blocky particles, but as coarse globules as well as finer but blocky particles mixed with the $NbCr_2$ phase. The coarse globules are anarchically placed in the microstructure (either isolated or as aggregates of two to five or more). This suggests that these globules were among the first crystals to appear during solidification and they freely moved in the liquid before agglomeration into groups of several globules. There are also very white almost spheroidal particles but much smaller than the Nb solid solution globules. According to the EDS spot analyses carried out, these new particles are very rich in hafnium, niobium and carbon. By comparison with the three previous alloys, new peaks are present in the diffractograms: they correspond to the NbC crystalline structure (cubic, space group: Fm-3m). The presence of these new particles and of these new peaks suggests that the spherical particles are MC carbides (M=Nb and Hf), with the same crystalline structure as NbC. With an average number higher than the Nb solid solution, these small globular Nb(Hf)C are the new whitest phase present when the microstructure is observed in BSE mode (the Nb solid solution globules become bright grey with a new contrast/brightness rating). Furthermore, these small Nb(Hf)C particles are either isolated or attached to a Nb solid solution globule (Fig. 7). One can also observe the presence of small Nb(Hf)C particles included in the Nb globules. It is possible to envisage that each Nb globule is associated with a small Nb(Hf)C particle either attached to its surface or included in its volume, since the Nb(Hf)C are visible only if the observation section crosses these particles. The position of these white Nb(Hf)C spot by respect to the Nb globules suggests that these small Nb(Hf)C small particles crystallized first at the solidification beginning, and served as substrates for the nucleation of the Nb globules. Such facilitated nucleation at the beginning of solidification may lead to much more crystals of Nb solid solution which did not grow longer after. This may explain the morphologic difference of the pre-eutectic Nb phase here by comparison to the three other alloys for each nucleation was probably less easy with as consequence more time for growth then to develop solid/liquid instabilities leading to a dendritic shape for crystals.

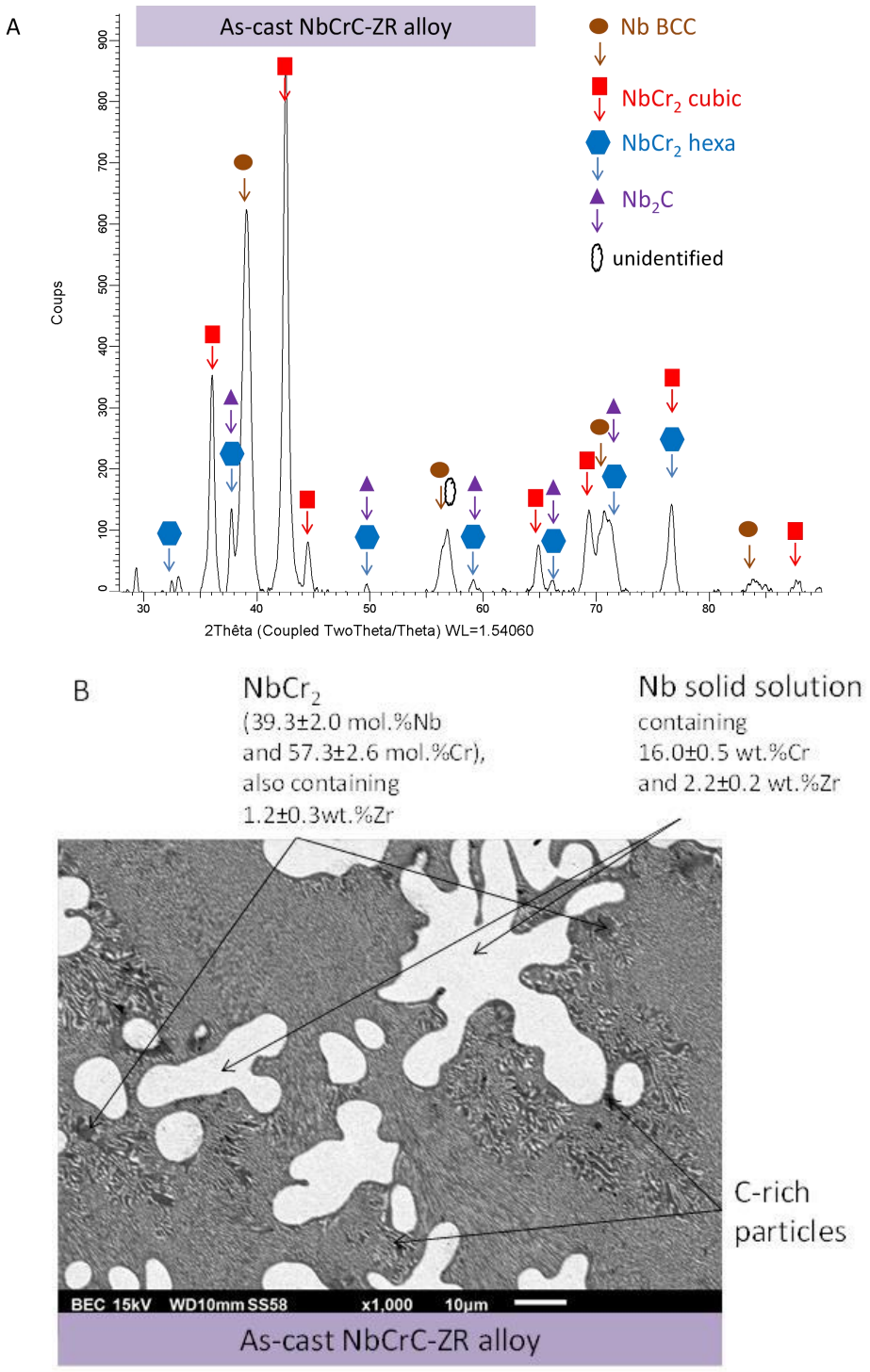

Figure 5; Zr-containing alloy: XRD diffractometer (A) and detailed view of its microstructure (B) with identification of the present phases (SEM/BSE micrograph)**.**

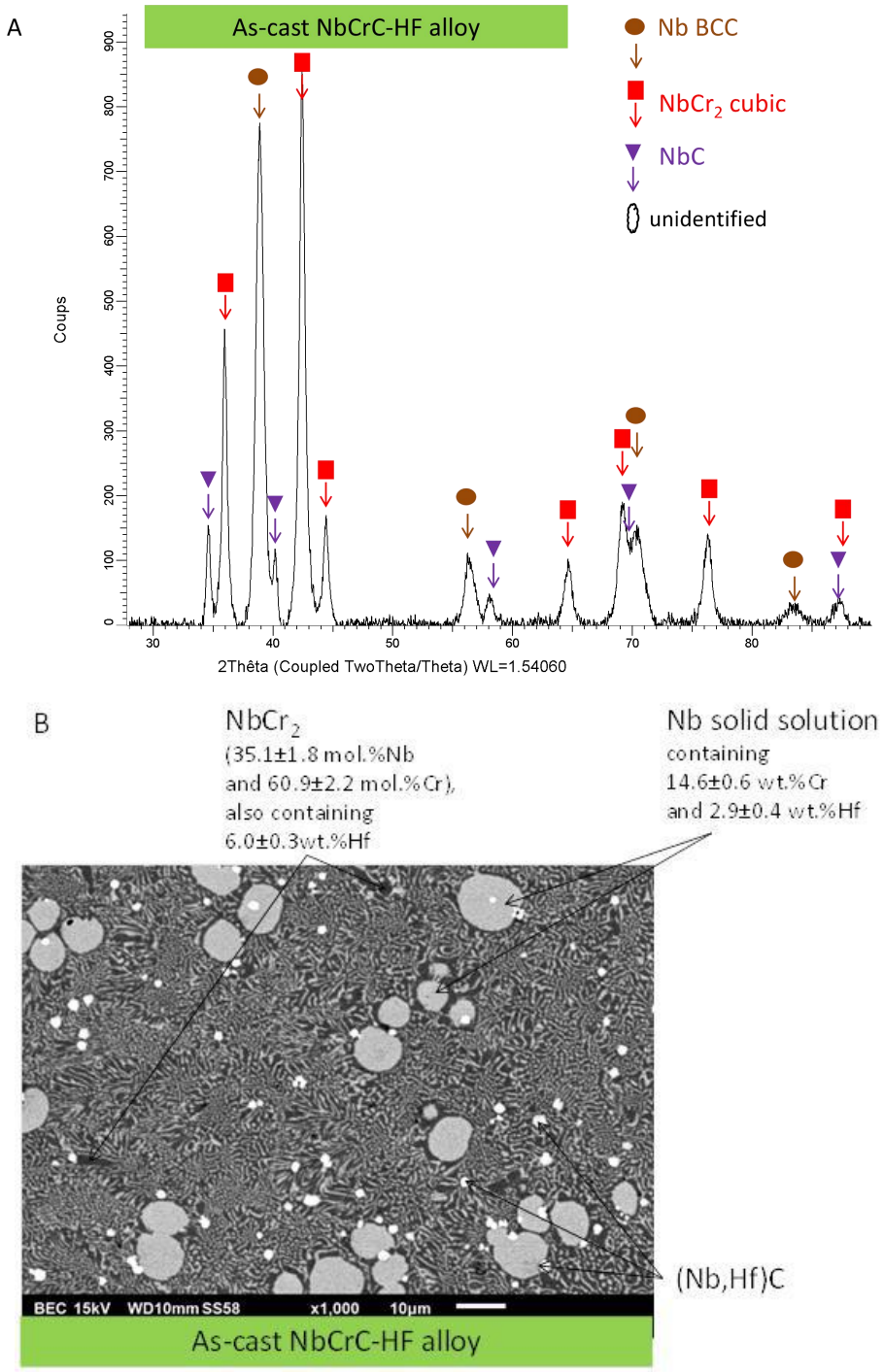

Figure 6; Hf-containing alloy: XRD diffractometer (A) and detailed view of its microstructure (B) with identification of the present phases (SEM/BSE micrograph)**.**

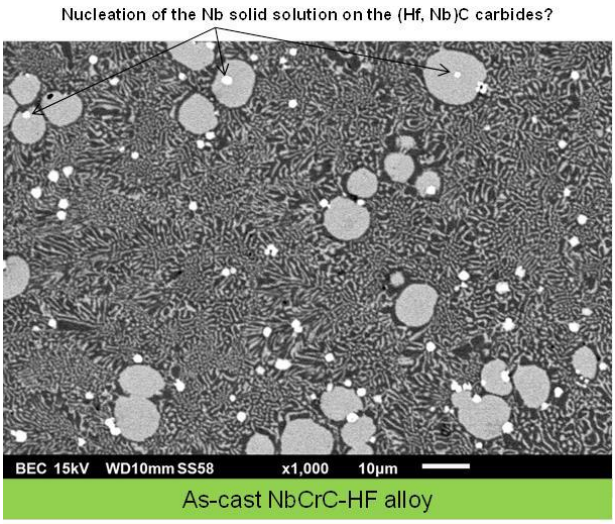

Figure 7; Hf-containing alloy: high magnification (×1000) view of the interactions of the Nb globules and the small round HfC (SEM/BSE micrograph)**.**

Vickers indentation

A series of ten Vickers indentations were performed in each alloy with an applied load equal to 10kg. This led to the average values given in Table 1, together with the values of the corresponding standard deviations. One can see that the room temperature hardness of the four alloys is very high. The Ta-containing alloy and the Ti-containing one both present hardness values higher than 1000 HV. The Hf-containing alloy and the Zr-containing one are only a little less hard than the two formers, with about 900 HV.

ALLOY NAME	**Hardness (HV10kg)**	**AVERAGE VALUE**	**Standard deviation**
NbCrC-TA		1038	67
NbCrC-TI		1005	82
NbCrC-ZR		915	28
NbCrC-HF		886	42

Table 1. Average and standard deviation of the Vickers hardness of each alloy (ten indentation per alloy, 10 kg load)

When one examines the alloys using the SEM in Secondary Electrons (SE) mode, one observes that cracks almost systematically propagated from the corners of the Vickers marks (pyramids), or from the neighborhood of these corners, for the four alloys. Two SEM/SE pictures of Vickers marks with cracks (here: in the "hard" Ta- and "soft" Zr-containing alloys) and two pictures without cracks (here: in the "hard" Ti- and "soft" Hf-containing alloys) are displayed in **Figure 8** for illustrating that. For a given alloy, the great majority of Vickers marks are concerned by cracks initiation but there are some without cracks. These cracks crossed independently the white Nb phase and the grey eutectic. Since the dimensions of the pyramids obtained by indentation may be a little higher when cracks occurred than in the opposite case, values a little scattered were obtained with as result standard deviations rather important.

Because it can be thought that the ratio between the two main phases, BCC Nb-based solid solution and $NbCr_2$, may be responsible of the difference in hardness of the four alloys image analysis was carried out on three ×1000 SEM/BSE microphotos to specify the surface areas of the BCC Nb phase, the surface fraction of $NbCr_2$ being considered as the complementary part taking into account that the Nb_2C, Nb(Hf)C and C-rich particles each represent a much lower surface fraction. The possible dependence of hardness on the Nb phase / $NbCr_2$ proportion can be studied in Fig. 9 in which the average hardness ± standard deviation is plotted versus the average surface fraction of the Nb phase (Table 2).

ALLOY NAME	**BCC Nb-phase surface fraction**	**AVERAGE VALUE**	**Standard deviation**
NbCrC-TA		57.7	8.3
NbCrC-TI		31.5	7.5
NbCrC-ZR		48.2	5.4
NbCrC-HF		27.0	9.7

Table 2. Average and standard deviation of the surface fraction of BCC-Nb phase present in each alloy (three image analyses per alloy)

Despite the rather high difference in Vickers hardness between the two major phases (about 1320 for BCC Nb-phase[28] and about 870 for $NbCr_2$[29] whatever its crystalline structure C14 or C15) no systematic increase in hardness can be seen, even if there is a tendency for that. This can be explained by the difficulty to measure the surface fraction of the part of Nb phase mixed with the $NbCr_2$ (rather fine particles and thus problem of rating and thus of accuracy), or by a possible important role of the size and morphology of the Nb phase which are not exactly the same between the alloys.

One can also mention, as possible cause of absence of clear dependence, the presence of either Ta, either Ti either Zr or either Hf in substitution in both phases.

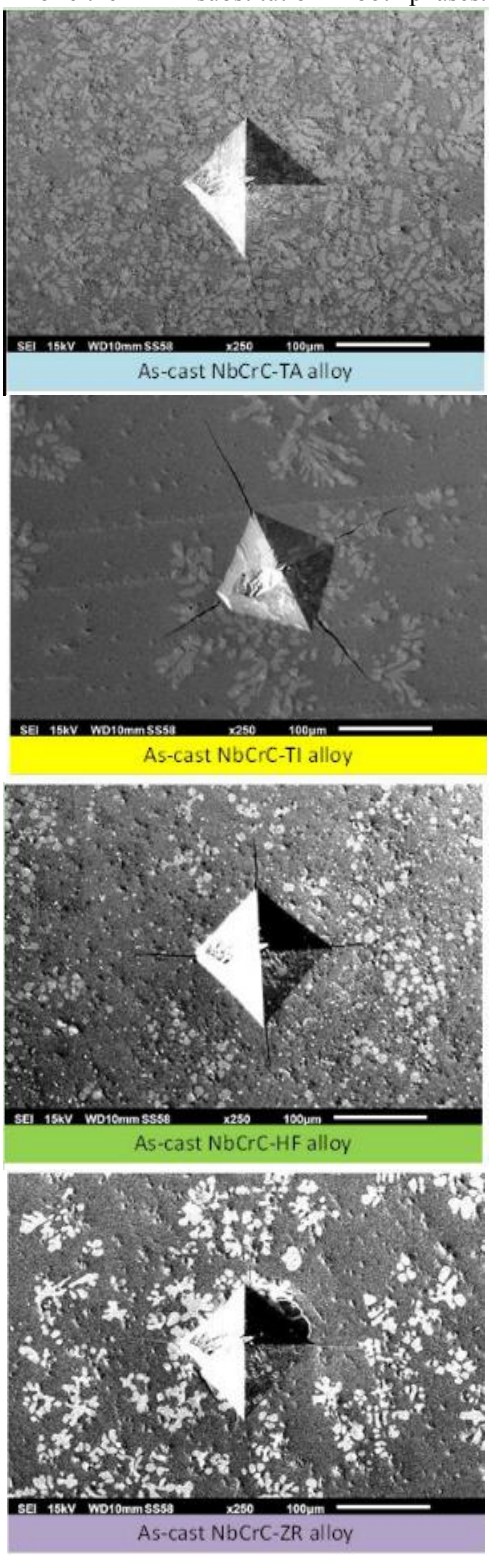

Figure 8; All alloys: illustration of the possible presence of cracks formed from the indentation marks (SEM/BSE micrographs)**.**

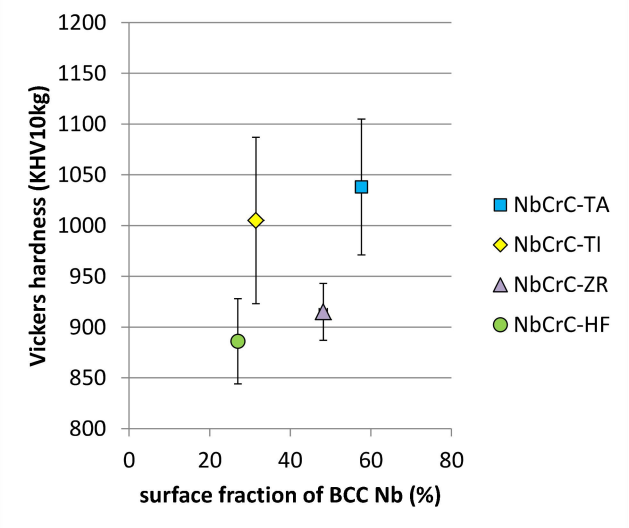

Figure 9; All alloys: illustration of the possible presence of cracks formed from the indentation marks (SEM/BSE micrographs)**.**

4. Summary and conclusions

In contrast with cobalt-based, nickel-based and iron-based alloys with similar contents in Cr, C and the same MC-former elements, and synthesized using the same apparatus and following similar protocols, the niobium-based alloys did not present the same as-cast microstructures. Notably, no script-like eutectic MC carbides were obtained in the interdendritic spaces of the alloys with a dendritic Nb-based solid solution matrix. There is an exception, Hf, since small round HfC precipitated and maybe acted as nuclei for the Nb solid solution globules of the Hf-containing alloy. Globally the four alloys were effectively constituted on a matrix made of a bcc solid solution of Nb (containing all almost the same content in chromium), and a significant proportion of the M element) and of a rather extended eutectic compound combining a Laves phase $NbCr_2$ and a part of the Nb solid solution. This explains the high values of hardness and the brittle mechanical behavior at room temperature. This is rather surprising to see graphite, even in very small quantity, in presence of so high cumulated content in carbide-forming elements, more precisely MC-forming for many of them (including Nb itself). In one case Nb_2C precipitated at solidification instead NbC, what can be understood considering the high Nb/C atomic ratio.

These new metallurgical systems seem being interesting to further investigate under the academic

point of view. Thermodynamic modelization in the theoretic field and quenching during directional solidification can be envisaged for a better understanding and description of the successive precipitation stages during solidification. Future work will consist to study, at elevated temperature, how these microstructures may evolve and what are their mechanical strength.

Obtaining new alloys extrapolated from these systems and presenting the required room temperature machinability and all temperatures minimal ductility, supposes complexifying their chemical compositions with the addition of elements able to correct this problematic brittleness.

References

1. Sims CT, Hagel WC(Eds.), The superalloys, John Wiley & Sons, Inc, New York, 1972.
2. Donachie MJ, Donachie SJ(Eds.), Superalloys: a technical guide (2nd edition), ASM International, Materials Park, 2002.
3. Nembach E, Neite G, Precipitation hardening of superalloys by ordered γ'- particles, Progress in Materials Science 29 (1985) 177-319.
4. Klauke M, Mukherji D, Gorr B , *et al*, Oxidation behaviour of experimental Co-Re-base alloys in laboratory air at 1000°C, International Journal of Materials Research (formerly Z. Metallkd.) 100 (2009) 104-111.
5. Gorr B, Burk S, Depka T, *et al*, Effect of Si addition on the oxidation resistance of Co-Re-Cr-alloys: recent attainments in the development of novel alloys, International Journal of Materials Research (formerly Z. Metallkd.) 103 (2012) 24-30.
6. Cui C , Ping D, Gu Y, *et al*, A new Co-base superalloy strengthened by γ' phase, Materials Transactions 47 (2006) 2099-2102.
7. Mishra B, Ionescu M, Chandra T, Feasability of cast and wrought Co-Al-W-X gamma prime superalloys, Materials Science Forum 783-786 (2013) 1159-1164.
8. Gorr B, Azim M, Christ H-J , *et al*, Microstructure evolution in a new refractory high entropy alloy W-Mo-Cr-Ti-Al, Metallurgical and Materials Transactions A: Physical Metallurgy and Materials Science 47 (2016) 961-970.
9. Berthod P, High temperature properties of several chromium-containing Co-based alloys reinforced by different types of MC carbides (M = Ta, Nb, Hf and/or Zr), Journal of Alloys and Compounds, 481 (2009) 746-754.
10. Berthod P, Conrath E, As-cast microstructures and behavior at high temperature of chromium-rich cobalt-based alloys strengthened by hafnium carbides, Materials Chemistry and Physics, 143 (2014) 1139-1148.
11. Conrath E, Berthod P, Microstructure Evolution at High Temperature of Chromium-Rich Iron-based Alloys containing Hafnium Carbides, International Journal of Materials Research (formerly Z. Metallkd.), 105 (2014) 717-724.
12. Berthod P, Conrath E, Microstructure evolution in the bulk and surface states of chromium-rich nickel-based cast alloys reinforced by hafnium carbides after exposure to high temperature in air, Materials at High Temperature, 31 (2014) 266-273.
13. Berthod P, Conrath E, Creep and oxidation kinetics at 1100°C of nickel-base alloys reinforced by hafnium carbides, Materials and Design, 104 (2016) 27-36.
14. Berthod P , Conrath E , Mechanical and Chemical Properties at High Temperature of {M-25Cr}-based Alloys Containing Hafnium Carbides (M=Co, Ni or Fe): Creep Behavior and Oxidation at 1200°C, Berthod P, Conrath E, Journal of Materials Science and Technology Research, 1 (2014) 7-14.
15. Berthod P, Looking for new polycrystalline MC-reinforced cobalt-based superalloys candidate to applications at 1200°C, Advances in Materials Science and Engineering, *in press*.
16. Berthod P , New polycrystalline MC-reinforced nickel-based superalloys for use at elevated temperatures (T >1100°C), Advanced Materials Letters, *submitted*.
17. Shaffer PTB, High Temperature Materials. N°1 Materials Index, Plenum Press, New York, 1964.
18. Sims CT , Niobium in superalloys: a perspective, High Temperature Technology, 2 (1984) 185-201.
19. Dropmann MC, Stover D, Buchkremer HP, *et al*, Properties and processing of niobium superalloys by injection molding, Advances in Powder Metallurgy and Particulate Materials 8 (1992) 213-224.
20. Young D, High Temperature Oxidation and Corrosion of Metals, Elsevier, Amsterdam (2008).
21. Zhai Y, Lados DA, Brown EJ , *et al*, Fatigue crack growth behavior and microstructural mechanisms in Ti-6Al-4V manufactured by laser engineered net shaping, International Journal of Fatigue 93 (2016) 51-63.
22. Baldan A , Microstructural investigation of DS200 + hafnium superalloy, Zeitschrift für Metallkunde, 80 (1989) 635-642.
23. Kotval PS, Venables JD , Calder RW , Role of hafnium in modifying the microstructure of cast nickel-base superalloys, Metallurgical transactions, 3 (1972) 453-458.
24. Murata Y , Suga K , Yukawa N, Effect of transition elements on the properties of MC carbides in IN-100 nickel-based superalloy, Journal of Material Science 21 (1986) 3653-3660.
25. Opiekun Z, Influence of zirconium and heat treatment on the structure of heat-resistant cobalt casting alloys of MAR-M509 type, Journal of Material Science, 22 (1987) 1547-1556.

26. Tsai YL, Wang SF, Bor HY , *et al*, Effect of Zr addition of the microstructure and mechanical behavior of a fine-grained nickel-based superalloy at elevated temperature. Materials Science and Engineering A: Structural Materials: Properties, Microstructure and Processing, 607 (2014) 294-201.
27. Paul H , Darrieulat M , Vanderesse N, *et al*, Microstructyure of warm worked Zircalloy-4, Archives of Metallurgy and Materials, 55 (2010) 1007-1019.
28. https://www.webelements.com/niobium/physics.html
29. Zhu JH , Liu CT , Liaw PK , Phase stability and mechanical behavior of NbCr2-based Laves phases. Intermetallics, 7 (1999) 1011-1016.